Supporting Information

Few-layered Graphene-like Boron Nitride: A Highly Efficient Adsorbent for Indoor Formaldehyde Removal

Jiawei Ye[§], Xiaofeng Zhu[§], Bei Cheng, Jiaguo Yu* and Chuanjia Jiang*

State Key Laboratory of Advanced Technology for Materials Synthesis and Processing, Wuhan University of Technology, Luoshi Road 122, Wuhan 430070, P. R. China

[§]These authors contributed equally to this work.

*Corresponding authors.

Tel.: 0086-27-87871029, Fax: 0086-27-87879468, E-mail: jiaguoyu@yahoo.com; jiangcj2016@yahoo.com

Total number of pages: 12.

This Supporting Information provides:

1. Materials characterization methods.

2. Procedures of HCHO adsorption experiments.

3. Modeling of HCHO adsorption kinetics and isotherms

4. Three tables and 10 figures.

Characterization. The phase structures of p-BN and c-BN were analysed by X-ray diffraction (XRD) (Rigaku D/Max-RB, Japan) with Cu K_α radiation at a scan rate (2θ) of 0.05 °/s. The morphology of p-BN was observed by a field-emission scanning electron microscope (FESEM) (JEOL 7500F, Japan) at an accelerating voltage of 15 kV. Transmission electron microscopy (TEM) and high-resolution TEM (HRTEM) images were collected on a JEM-2100F microscope at an accelerating voltage of 200 kV. X-ray photoelectron spectra (XPS) measurements were carried out on VG ESCALAB210 with Mg K_α source. All binding energies were referenced to the C 1s peak at 284.8 eV of surface adventitious carbon. Fourier transform infrared (FTIR) spectra were collected using a Shimadzu IRAffinity-1 FTIR spectrometer in the range of 500–4000 cm^{-1}.

The Brunauer-Emmett-Teller (BET) specific surface area (S_{BET}) of the samples was determined by a multipoint method using N_2 adsorption data in the relative pressure (P/P_0) range of 0.05–0.3 (Micromeritics ASAP 2020, USA). Prior to N_2 adsorption measurements, all samples were degassed at 180 ℃. The pore size distributions were determined by the N_2 adsorption volume via the Barret-Joyner-Halender (BJH) method assuming a cylindrical pore model. The pore volume and the average pore size were estimated from the N_2 adsorption volume at P/P_0 of 0.994.

In situ diffuse reflectance infrared Fourier transform spectroscopy (DRIFTS) was performed on Thermo Fisher Nicolet iS50 FTIR Spectrometer. Prior to the DRIFTS tests, the adsorbent was purged with pure oxygen (O_2) gas for 120 min. Then a gas

mixture of HCHO + O_2 was introduced into the DRIFTS cell at room temperature and a flow rate of 30 mL/min. All spectra were recorded with a resolution of 4 cm^{-1}, and the background spectrum was subtracted from each spectrum.

HCHO adsorption test. HCHO adsorption experiments of the tested materials were performed in the dark and at 25 ℃ in a 6-L organic glass box reactor covered with aluminium foil on its inner walls. The adsorbent (50 mg) was dispersed on the bottom of a glass Petri dish (10 cm diameter), which was subsequently placed in the reactor and covered with a glass slide. Then 6 μL of concentrated HCHO solution (38 wt%) was injected into the reactor, and a 5 W fan near the bottom of reactor was turned on to accelerate the volatilization of HCHO. After 2 h, the HCHO solution was completely volatized and the concentration of HCHO stabilized at 151±3 parts per million (ppm). The HCHO adsorption experiment was started by removing the glass slide cover, and the real-time concentrations of HCHO, carbon dioxide (CO_2), carbon monoxide (CO) and water vapor were online detected by a Photoacoustic Field Gas Monitor (INNOVA AirTech Instruments, Model 1412). In the recycle experiments to test the performance stability, the adsorbents were heated by an infrared lamp for 30 min before subsequent HCHO adsorption tests. For measuring the adsorption isotherms of the p-BN and c-BN samples, initial HCHO concentrations ranged from 20 to 646 ppm.

The amount of HCHO adsorption, q_t (mg/g), at time t was calculated using equation (1):

$$q_t = \frac{(C_0 - C_t)V}{W} \quad (1)$$

where C_0 and C_t (mg/L) are the initial HCHO concentration and HCHO concentration at time t, respectively, V is the total volume of air in the reactor (V = 6 L), and W is the mass of the adsorbent (W = 0.050 g).

The equilibrium adsorption capacity of the samples, q_e, was calculated using equation (2):

$$q_e = \frac{(C_0 - C_e)V}{W} \quad (2)$$

where (C_e, in mg/L) is HCHO concentration measured at equilibrium (i.e., when the change in C_t was less than 0.5%).

Modeling of HCHO adsorption kinetics and isotherms. The adsorption kinetics of HCHO on the p-BN samples were fitted using pseudo-first-order and pseudo-second-order kinetic models. The linearized forms of the pseudo-first-order and pseudo-second-order kinetics equations are expressed as follows[1]:

Pseudo-first-order: $\ln(q_e - q_t) = \ln q_e - k_1 t$ (3)

Pseudo-second-order: $\frac{t}{q_t} = \frac{1}{k_2 q_e^2} + \frac{1}{q_e} t$ (4)

where k_1 (1/min) and k_2 (g/mg/min) are the rate constants of pseudo-first-order and pseudo-second-order adsorption, respectively, and q_e is the calculated equilibrium adsorption capacity.

The adsorption isotherms of HCHO on the p-BN and c-BN samples were fitted to the Langmuir and Freundlich isotherm models, using the linearized equations[1]:

$$\text{Langmuir:}\quad \frac{C_e}{q_e} = \frac{1}{q_m} C_e + \frac{1}{q_m K_L} \tag{5}$$

$$\text{Freundlich:}\quad \ln q_e = \frac{1}{n} \ln C_e + \ln K_F \tag{6}$$

where K_L is the Langmuir constant (L/mg), and q_m is the maximum adsorption capacity of the adsorbent (mg/g), while K_F and n are Freundlich constants related to the adsorption capacity and adsorption intensity, respectively.

Table S1. Sources of commercial materials.

Sample	Manufacturer
c-BN	Aladdin Industrial Corporation
AC	Tianjin kwangfu Technology Co., Ltd.
TiO_2 (P25)	Degussa AG
γ-Al_2O_3	Aladdin Industrial Corporation
SiO_2	Aladdin Industrial Corporation
α-Fe_2O_3	Aladdin Industrial Corporation
CeO_2	Aladdin Industrial Corporation
Molecular Sieve (13X)	Sinopharm Chemical Reagent Co., Ltd
Co_2O_3	Shantou Guanghua Chemical Plant

Table S2. Kinetic parameters for HCHO adsorption by p-BN sample.

	pseudo-first-order			pseudo-second-order		
$q_{e,exp}$ (mg/g)	k_1 (1/min)	$q_{e,cal}$ (mg/g)	R^2	k_2 (g/mg/min)	$q_{e,cal}$ (mg/g)	R^2
19.06	0.0995	9.38	0.9706	0.0228	19.84	0.9997

Table S3. In situ DRIFTS band assignments of adsorbed species on p-BN within the wavenumber range of 3000–1300 cm^{-1}. [a]

Species	Wavenumber (cm^{-1})	Assignment [b]	Literature value (cm^{-1})
Formate	2986	ν_{as}(COO) +δ(CH)	2991,[2] 2980,[3] 2956,[4] 2955[5]
	2863	ν(CH)	2868,[4] 2865,[6] 2864[7]
	2750	ν(CH)	2740[4]
	1610	$\nu_{as}(COO)_{(monodentate)}$	1612,[8] 1614[9]
	1566	$\nu_{as}(COO)_{(bidentate)}$	1570,[4] 1569[10]
	1371	δ(CH)	1380,[10] 1371[7]
Methoxy	2912	$\nu_{as}(CH_3)$	2926[5]
	2804	$\nu_s(CH_3)$	2820[5]
	1467	ν(CH)	1460[5]
Formaldehyde	1771, 1700	ν(C=O)	1770, 1715[3]
	1413	N/A [c]	1413[11]

Notes: [a] Broad bands at 3200–3600 cm^{-1} due to the stretching vibration of hydroxyl groups[9] are not included. [b] The symbols represent different vibration modes: δ, bending vibration; ν, stretching vibration; ν_{as}, asymmetric stretching vibration; ν_s symmetric stretching vibration. [c] Band assignment not available from the literature.

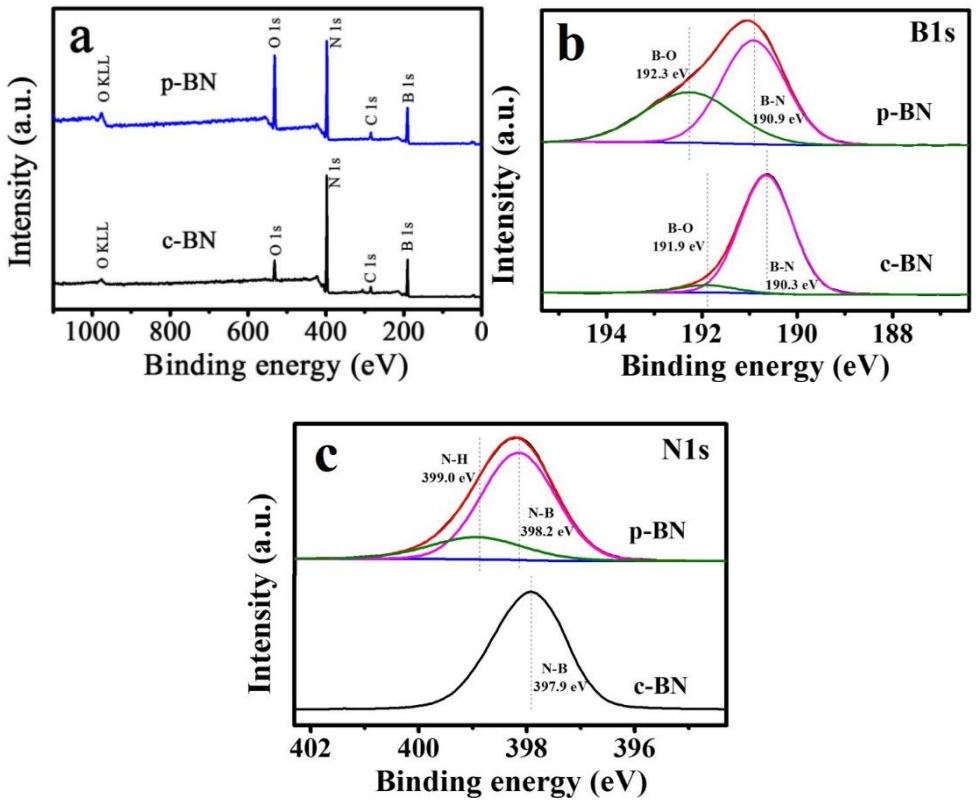

Figure S1. XPS survey spectra (a), high-resolution B 1s spectra (b) and N 1s spectra (c) of p-BN and c-BN samples.

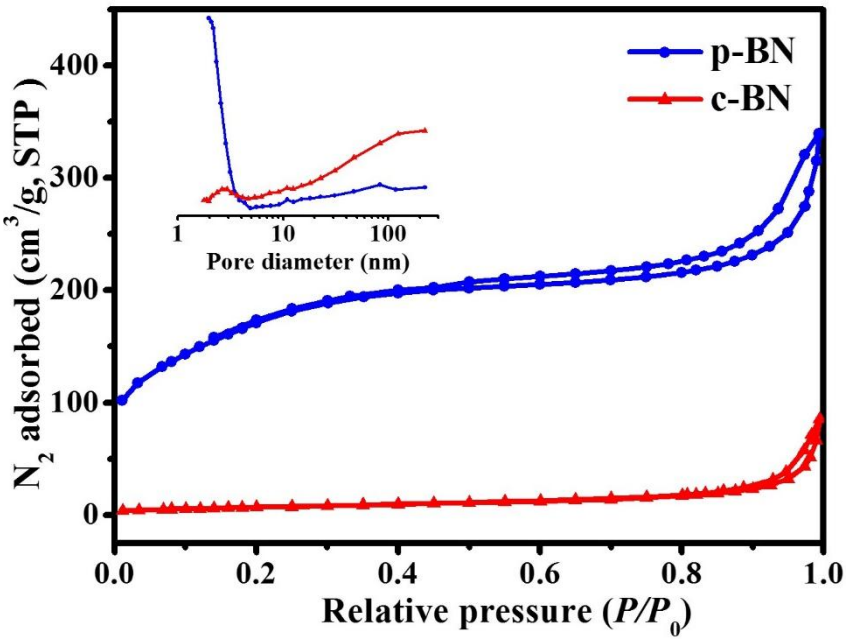

Figure S2. N_2 adsorption-desorption isotherms and the corresponding pore size distributions (inset) of the p-BN and c-BN samples.

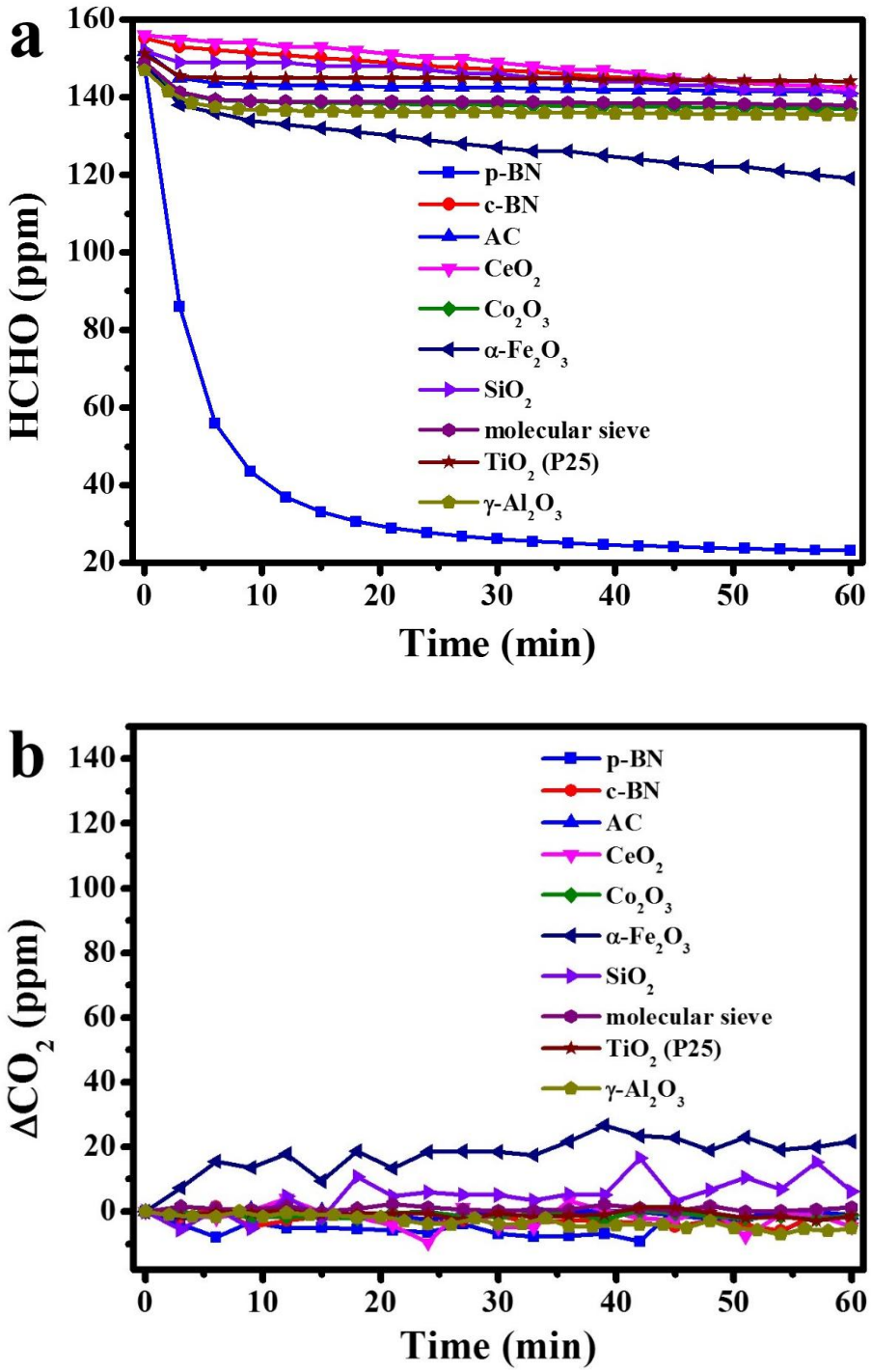

Figure S3. Changes of HCHO concentration (a) and ΔCO_2 (CO_2 concentration change relative to background level) (b) over time in the presence of p-BN and the commercial materials.

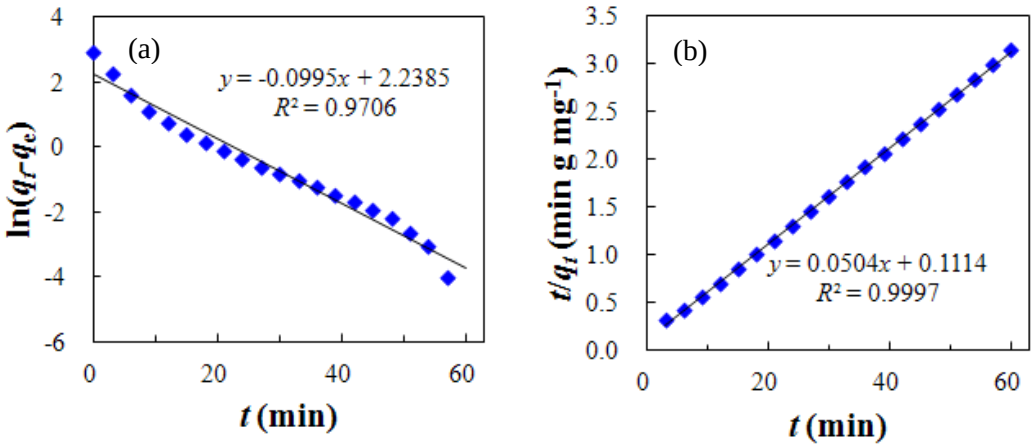

Figure S4. Modeling of HCHO adsorption kinetics by the p-BN sample using (a) pseudo-first-order and (b) pseudo-second-order kinetic models.

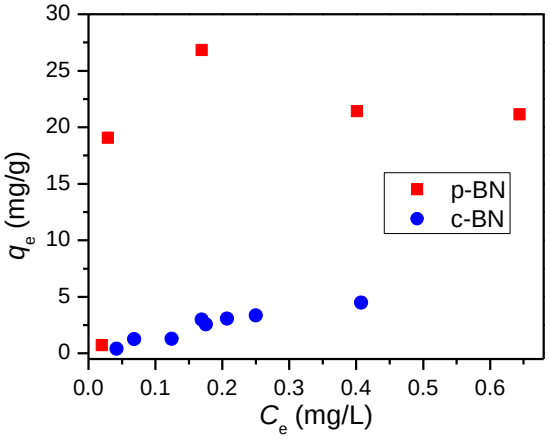

Figure S5. HCHO adsorption isotherms by p-BN and c-BN samples at room temperature.

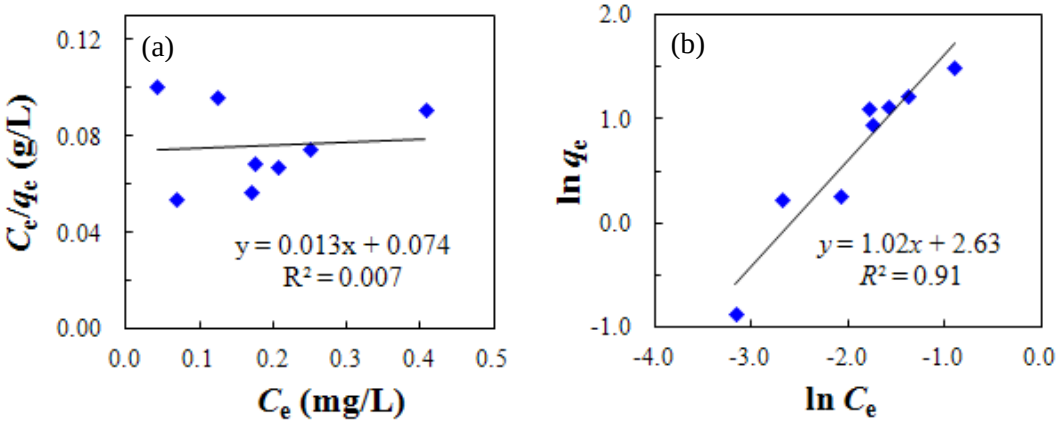

Figure S6. Data fitting of HCHO adsorption isotherm by c-BN using (a) Langmuir and (b) Freundlich isotherm models.

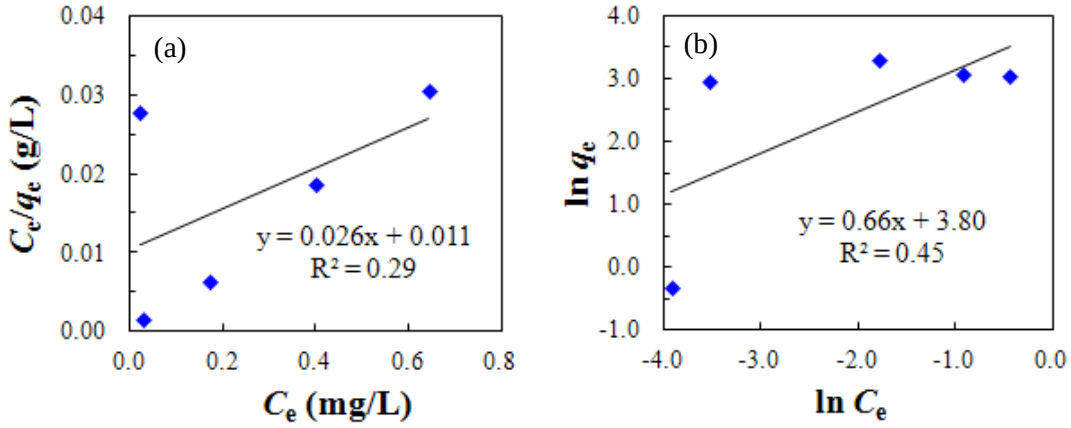

Figure S7. Data fitting of HCHO adsorption isotherm by p-BN using (a) Langmuir and (b) Freundlich isotherm models.

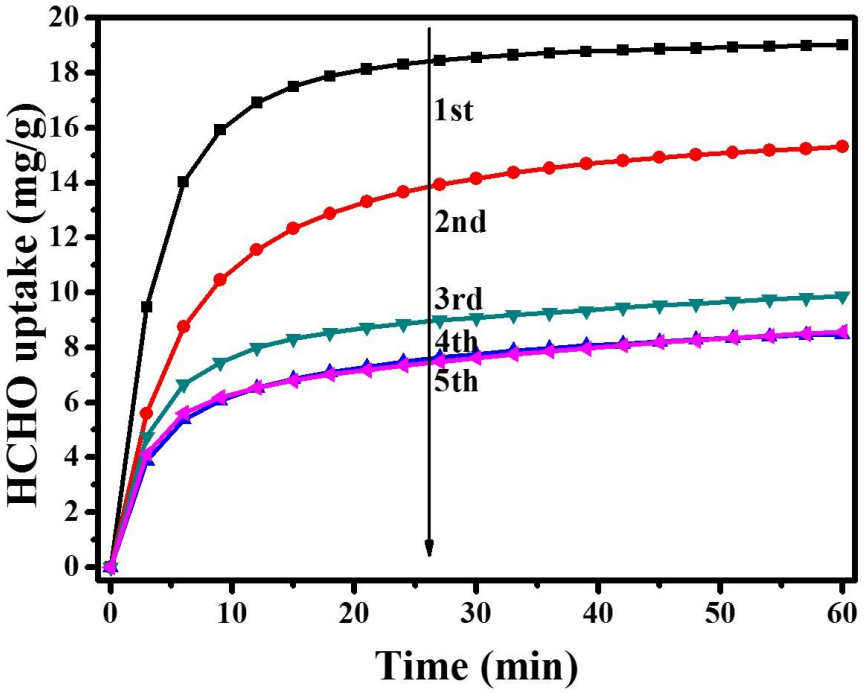

Figure S8. HCHO uptake as a function of time for the p-BN sample in recycling tests.

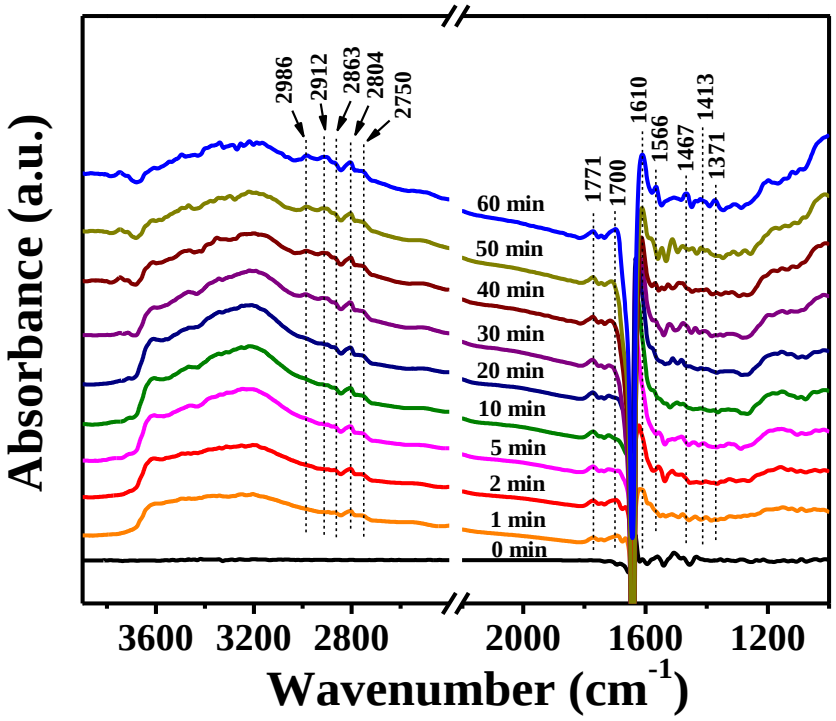

Figure S9. In situ DRIFTS spectra of p-BN adsorbent as a function of time under a flow of HCHO/O_2 at ambient temperature.

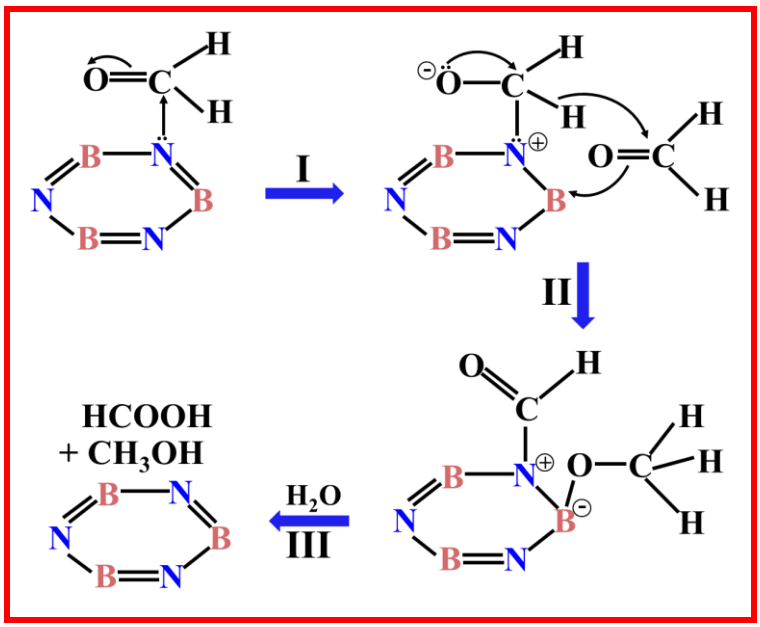

Figure S10. Proposed disproportionation reaction mechanism for HCHO over the surface of p-BN.

References

1. Xu, J.; Wang, L.; Zhu, Y. F., Decontamination of bisphenol A from aqueous solution by graphene adsorption. *Langmuir* **2012,** *28*, 8418-8425.
2. Collins, S. E.; Baltanas, M. A.; Bonivardi, A. L., An infrared study of the intermediates of methanol synthesis from carbon dioxide over Pd/beta-Ga_2O_3. *J. Catal.* **2004,** *226*, 410-421.
3. Chen, D.; Qu, Z. P.; Sun, Y. H.; Gao, K.; Wang, Y., Identification of reaction intermediates and mechanism responsible for highly active HCHO oxidation on Ag/MCM-41 catalysts. *Appl. Catal. B-Environ.* **2013,** *142*, 838-848.
4. Zhang, C. B.; He, H.; Tanaka, K., Catalytic performance and mechanism of a Pt/TiO_2 catalyst for the oxidation of formaldehyde at room temperature. *Appl. Catal. B* **2006,** *65*, 37-43.
5. Kattel, S.; Yan, B. H.; Yang, Y. X.; Chen, J. G. G.; Liu, P., Optimizing binding energies of key intermediates for CO_2 hydrogenation to methanol over oxide-supported copper. *J. Am. Chem. Soc.* **2016,** *138*, 12440-12450.
6. Qi, L. F.; Cheng, B.; Yu, J. G.; Ho, W. K., High-surface area mesoporous Pt/TiO_2 hollow chains for efficient formaldehyde decomposition at ambient temperature. *J. Hazard. Mater.* **2016,** *301*, 522-530.
7. Quiroz, J.; Giraudon, J. M.; Gervasini, A.; Dujardin, C.; Lancelot, C.; Trentesaux, M.; Lamonier, J. F., Total oxidation of formaldehyde over MnO_x-CeO_2 catalysts: The effect of acid treatment. *ACS Catal.* **2015,** *5*, 2260-2269.
8. Yan, Z. X.; Xu, Z. H.; Yu, J. G.; Jaroniec, M., Highly active mesoporous ferrihydrite supported Pt catalyst for formaldehyde removal at room temperature. *Environ. Sci. Technol.* **2015,** *49*, 6637-6644.
9. Ma, Y.; Zhang, G. K., Sepiolite nanofiber-supported platinum nanoparticle catalysts toward the catalytic oxidation of formaldehyde at ambient temperature: Efficient and stable performance and mechanism. *Chem. Eng. J.* **2016,** *288*, 70-78.
10. Wang, J. L.; Zhang, P. Y.; Li, J. G.; Jiang, C. J.; Yunus, R.; Kim, J., Room-temperature oxidation of formaldehyde by layered manganese oxide: Effect of water. *Environ. Sci. Technol.* **2015,** *49*, 12372-12379.
11. Sun, S.; Ding, J. J.; Bao, J.; Gao, C.; Qi, Z. M.; Li, C. X., Photocatalytic oxidation of gaseous formaldehyde on TiO_2: An in situ DRIFTS study. *Catal. Lett.* **2010,** *137*, 239-246.